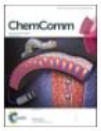

From the journal:
Chemical Communications

Towards single-molecule in situ electrochemical SERS detection with disposable substrates

Daniel Martín-Yerga, Alejandro Pérez-Junquera, María Begoña González-García, David Hernandez-Santos and Pablo Fanjul-Bolado

TOC entry

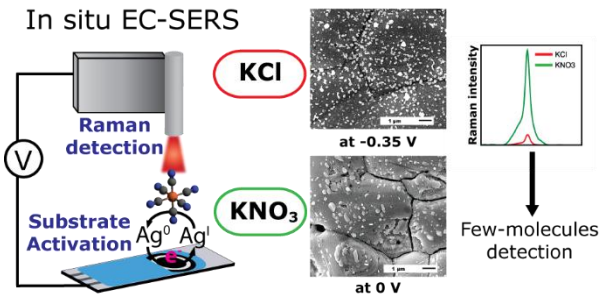

Nanostructure and surface charge can be tuned during the electrochemical activation of SERS substrates achieving highly active surfaces with feasible detection of a few molecules.

ChemComm

COMMUNICATION

Towards single-molecule *in situ* electrochemical SERS detection with disposable substrates

Received 00th January 20xx,
Accepted 00th January 20xx

DOI: 10.1039/x0xx00000x

www.rsc.org/

Daniel Martín-Yerga, Alejandro Pérez-Junquera, María Begoña González-García, David Hernández-Santos, Pablo Fanjul-Bolado*

Dynamic time-resolved Raman spectroelectrochemistry demonstrates the strong influence of the nanostructuring and surface charge of *in situ* activated disposable substrates for SERS detection. In specific conditions, a large enhancement factor and estimated calculations agree with the feasible detection of only a few molecules, approaching the limit of single-entity detection.

Sensitive detection methods are currently essential to solve numerous analytical problems and will become indispensable in the future. Surface-enhanced Raman spectroscopy (SERS)[1] is a powerful technique that allows the detection of ultralow concentrations promoted by the enhancement of the Raman scattered emission when the analyte strongly interact with active metallic surfaces. This technique has been capable of single-molecule detection[2,3]. Detection of individual molecules could be valuable for understanding molecular processes and for future diagnostic applications[4] with excellent sensitivity. The assembly of high-activity SERS substrates has advanced significantly with the development of novel nanofabrication techniques[5], but electrochemistry has played a significant role since the discovery of this technique by Fleischmann[6]. The oxidation-reduction cycling (ORC) method is considered the universal method for the activation of silver surfaces used as SERS substrates[6–8]. There is a general consensus for using chloride-based electrolytes in this process because the initial oxidation of silver generates insoluble AgCl increasing the electrode roughening. However, it is well known that the plasmonic properties are strongly determined by the structural characteristics of the generated nanostructures such as shape, size, density or surface charge[9,10]. A universal method does not allow to control these surface properties, which could positively affect the SERS signal and make the electrochemical fabrication of SERS substrates competitive again.

DropSens S.L., Edificio CEEI, Parque Tecnológico de Asturias, 33428 Llanera, Spain.
**e-mail: pfanjul@dropsens.com*

Electronic Supplementary Information (ESI) available: [details of any supplementary information available should be included here]. See DOI: 10.1039/x0xx00000x

In this work, we demonstrate that the counter-anion during the ORC method with disposable silver substrates completely changes the SERS signal. Two factors can influence the SERS activity: the generation of different silver nanostructures and the substrate surface charge in the specific moment when the active structure is generated in presence of the analyte. The increased activity resulted in a large SERS enhancement factor (EF) and the detection of pM concentrations of the chemical probe, which agrees with the possible detection of only a few molecules, approaching the limit of single-entity detection. These findings challenge the consensus of using chloride-based electrolytes for the ORC as the universal electrochemical method for generation of sensitive SERS substrates.

Dynamic Raman spectroelectrochemistry was performed with simultaneous and *in situ* substrate activation and SERS detection, the so called electrochemical SERS (EC-SERS). Screen-printed silver electrodes were employed as the substrate due to their low-cost and disposability, which make them a versatile platform for decentralized point-of-care analysis. A single oxidation-reduction cycle was applied to activate the silver surface in presence of $1x10^{-5}$ M ferricyanide. Ferricyanide was chosen as a model species widely employed in SERS studies[11] as it shows strong bands above 2000 cm^{-1}. A complete Raman spectrum was *in situ* recorded every 2 s with a potential resolution of 100 mV allowing to get representative time-resolved information of the processes taking place on the surface during the substrate activation. We compared the SERS activation obtained using KCl, employed in the universal ORC method, and KNO_3, where the counter-anion does not generate insoluble species. Interestingly, we found a strong 9X enhancement of the SERS signal (**Figure 1A**) just by replacing the counter-anion employed during the activation (90100 vs 9930 counts). This fact was observed in other bands from ferricyanide (**Figure S1**), suggesting that the activity increased by the surface features and not by a change of the molecule orientation. Since

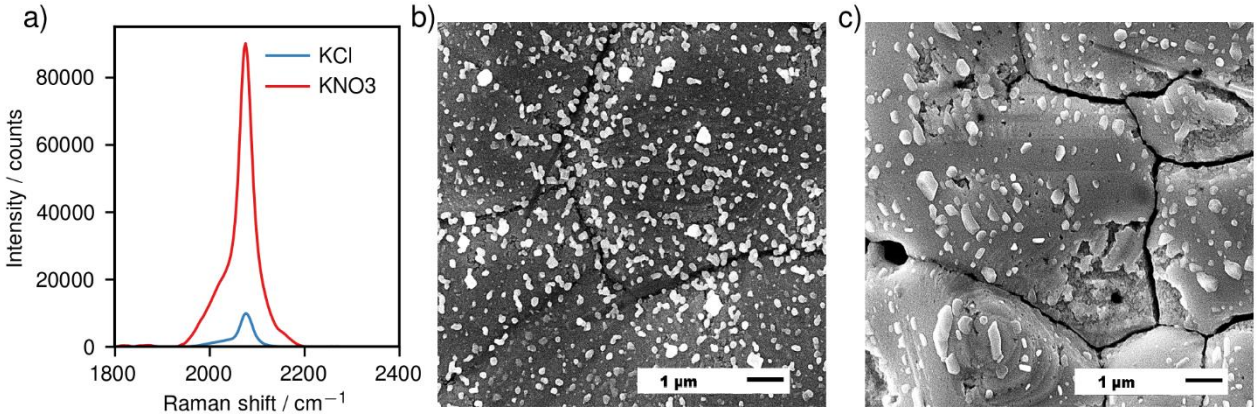

Figure 1. a) Highest SERS signal obtained for $1x10^{-5}$ M ferricyanide after the substrate activation in KCl and KNO_3. SEM images of the silver substrate obtained at the optimal point for the activation with b) KCl and c) KNO_3.

the discovery of the SERS effect[6], numerous studies have been reported using chloride-based electrolytes for the activation of silver substrates[6–8], being considered as the universal technique. However, this simple experiment shows that this method could not be the most appropriate in some cases and an increased sensitivity could be obtained with alternative electrolytes.

We tried to elucidate the effect of the structural properties of the surface by correlating the spectroelectrochemical information with surface imaging at different stages of the substrate activation. It is well-known that the electrolyte could have a decisive influence on the surface properties and that the SERS effect is widely affected by the shape, size and density of nanostructured particles[12,13]. **Figure 1B** shows typical scanning electron microscopy (SEM) images obtained for the silver substrate when the SERS signal is maximum with Cl^- or NO_3^- as counter-anions. Both surfaces were remarkably different and compared to the initial screen-printed surface (**Figure S2**). In presence of Cl^-, the substrate was most active when covered by silver nanoparticles (composition confirmed by energy-dispersive X-ray spectroscopy (EDX), **Figure S3**). In this case, silver chloride was initially generated during the oxidative stage (**Figure S4**). Although different nanoparticles could be observed over the surface, most of the particles were quasi-spherical. The size distribution was not particularly homogeneous but most particles were between 100 and 300 nm with some aggregates. SEM images of the silver surface activated in presence of NO_3^- showed flatter electrodeposited structures resembling silver nanoplatelets (**Figure 1C**). The more homogeneous colour contrast between the nanoplatelets and the electrode substrate suggests a low height of these structures compared to the other dimensions, although these properties are typically difficult to determine by SEM imaging. Different shapes for these nanoplatelets such as hexagons or rectangles are also observed, which clearly increases the density of particle edges compared to the quasi-spherical silver nanoparticles observed with KCl. As mentioned above, these properties have certainly some influence on the SERS signal and it has been previously proposed that the particle edge in contact with other structures is a region where hot spots could be formed[14,15], resulting in a higher signal enhancement. The size of the silver nanoplatelets was generally above 200 nm with many particles c.a. 500 nm, bigger than the nanoparticles generated with KCl. It has also been suggested that smaller silver nanoparticles do not exhibit high plasmonic activity required for SERS[16]. In this case, the oxidation step does not generate an insoluble product on the surface, and only a slight etching of the top layers of the electrode was observed (**Figure S5**). Although this process caused a visual increment of the roughness (and surface area), it did not result in any SERS signal (*vide infra*). This fact suggests that the etched surface is not SERS active. The high correlation between the generation of silver particles and the SERS activity indicates that the active area is only due to fresh particles. Therefore, we have demonstrated that the substrate activation can generate particles with different size and geometry, which definitely may have an influence on the recorded SERS signal.

The SERS effect is mainly explained by two possible events[17]: the electromagnetic enhancement (EM) and the chemical enhancement (CE). The predominant EM is mainly due to the plasmonic properties of the nanostructured surface, and the CE is due to changes on the molecule polarizability by a strong adsorption on the metallic surface. Electrochemistry is a really attractive technique to direct the CE of the SERS effect[18] because by controlling the surface charge, the adsorption of the probe molecule could be tuned[19]. *In situ* dynamic spectroelectrochemistry is excellent to detect small changes on these properties with a high potential-resolution. Therefore, we also tried to elucidate the effect of the surface charge on the SERS effect. **Figure 2** shows the potential-dependent evolution of the SERS signal during the dynamic experiments performed in KCl and KNO_3. No SERS effect was observed initially for the bare electrode or at the anodic potentials. The oxidation of the electrode in presence of KCl generates insoluble AgCl on the surface, which has been reported as not SERS-active[20]. In presence of KNO_3, the silver was etched, increasing the electrode roughness (visually observed in **Figure S5**). Although the roughening has been widely accountable for the SERS effect, this demonstrates that this process by itself does not enhance the Raman signal and the generation of specific active nanostructures is essential. The SERS signal significantly increased when the silver reduction took place in both cases, and achieved the maxima responses at the end of the silver

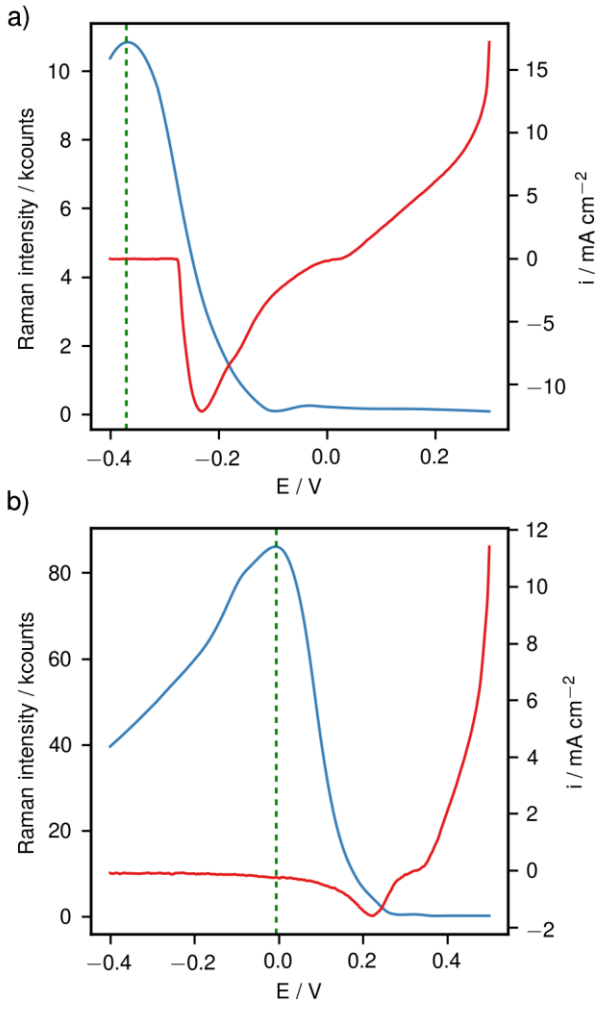

Figure 2. Evolution of the SERS response at 2076 cm^{-1} (blue line) for $1x10^{-5}$ M ferricyanide during the voltammetric activation (red line) of the silver substrate in a) KCl and b) KNO_3.

reduction. As expected, the cathodic peak potentials were different when using KCl or KNO_3 and the maximum SERS signal was obtained at -0.37 V and 0 V, respectively. The generation of insoluble AgCl results in a more difficult reduction of Ag^I to Ag^0, and the potential is negatively shifted compared to KNO_3. In the latter case, soluble Ag^+ is formed and the reduction to Ag^0 is achieved at more positive potentials. Therefore, the maximum SERS signals are obtained when the silver nanostructures are generated but at different potentials. The electrode potential strongly influences the sign and magnitude of the surface charge. The probe molecule (ferricyanide) is anionic and the adsorption with the silver surface can be significantly stronger at more positive potentials, which could enhance the SERS signal. The effect of the surface charge is again demonstrated by the signal decrease after the maximum when the surface charge becomes more negative and could repel the anionic probe. In order to confirm the effect of the surface charge in the SERS response, two different tests were performed: ferricyanide was again evaluated but using a different electrolyte that also form soluble silver species ($LiClO_4$), and the SERS effect of a cationic species ($[Ru(bpy)_3]^{2+}$) in KCl and KNO_3 was investigated (see **Figure S6** for complete discussion). The SERS signal for ferricyanide in $LiClO_4$ was higher than the one obtained in KCl, with the maximum signal also obtained at more positive potentials (0 vs -0.37 V). In contrast, the highest SERS signal for $[Ru(bpy)_3]^{2+}$ was observed when the activation was performed in KCl and the surface charge was more negative. These results are very attractive as the method could be tuned in order to generate the active silver nanoparticles at different potentials, enhancing the adsorption selectivity towards the detection of cationic or anionic species under different conditions. It is interesting to mention that the SERS signal in KNO_3 was higher than in $LiClO_4$ but the potential of the maximum SERS signal was similar. In this case, the structural features (**Figure S7**) of the fresh silver could also be essential to explain the different SERS activity. We should also consider that these results have been obtained using a 785 nm laser. It is well-known the importance of the laser wavelength on Raman spectroscopy[21,22], which could influence the chemical enhancement or produce resonant processes in the studied systems. Therefore, the results using other lasers could be different if other processes are involved.

Supported by the 9X increment of the SERS response with KNO_3 compared to the universal ORC method, we evaluated the limits of the SERS detection. Although the voltammetric method is the most employed for the electrode activation, we have demonstrated that the SERS signal depends strongly on the applied potential and the integration time can only be slightly increased in a sweep experiment to record one spectrum at the optimal potential range. To be able to increase the integration time, chronoamperometry was employed for the *in situ* electrochemical activation. Initially, an anodic potential (+0.4 V) was applied for 3 s to induce the silver oxidation and then a cathodic potential (0 V) was applied to reduce the oxidised silver while the Raman spectra were recorded. The integration time was increased to 8 s to achieve a more sensitive detection (incrementing the probability of detecting scattered photons). Under these conditions, a peak intensity like that obtained using voltammetry with integration time of 2 s for a $1x10^{-5}$ M solution was obtained for a solution of only $1x10^{-7}$ M. The enhancement factor (EF) was calculated according to the following equation[23]:

$$EF = \frac{I_{SERS} C_{Normal}}{I_{Normal} C_{SERS}} \quad (1)$$

where I_{SERS} and I_{Normal} are the intensities for the SERS and normal Raman spectra and C_{SERS} and C_{Normal} are the concentrations used in the experiments, respectively. The calculated EF was $1.8x10^8$, which demonstrates the strong enhancement obtained with the method and is considered to be sufficiently high for single-molecule measurements as previously discussed[14,24]. The relationship between the SERS intensity at 2076 cm^{-1} and the concentration of ferricyanide in solution shows the typical behavior of the SERS effect following a Langmuir adsorption isotherm (**Figure 3**). Therefore, it is reasonable to think that, at very low concentrations (first detectable concentration was $5x10^{-10}$ M), the active area could be in submonolayer coverage. The detection of ferricyanide at these ultralow concentrations using disposable electrodes is very interesting and it does not have any precedent in previous studies in the literature. Due to

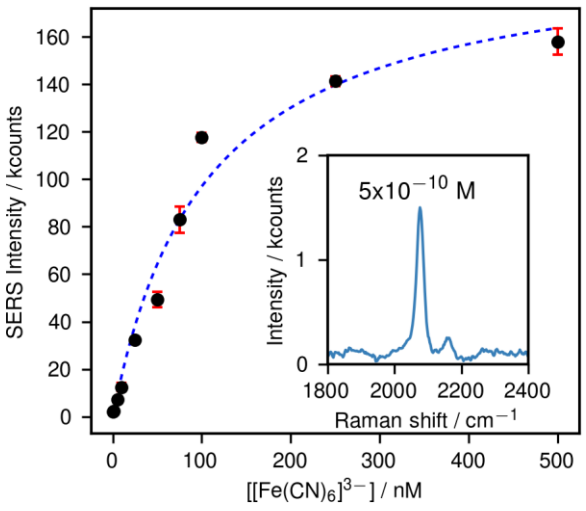

Figure 3. Relationship between the ferricyanide concentration in solution and the SERS intensity at 2076 cm^{-1}. The dashed blue line indicates the behaviour of the Langmuir adsorption isotherm. Inset shows the Raman spectrum obtained for the concentration of $5x10^{-10}$ M.

the high EF calculated and in order to consider the possible detection of single-molecule events, we performed a rough calculation to estimate the number of molecules being effectively irradiated under the experimental conditions for a concentration of $5x10^{-10}$ M ferrocyanide. The calculations and complete discussion are available in the Supporting Information. It was roughly estimated that less than 10 molecules could be available in the detectable region. Therefore, all the results suggest that the SERS signal could come from only a few molecules in the active region, which is impressive considering the simplicity of the experiments performed. To unequivocally confirm this fact, more complex studies are needed but this work is a first approach towards the detection of single or a few entities with *in situ* electrochemical SERS using disposable substrates, which could be very valuable to solve analytical problems with high sensitivity.

In conclusion, *in situ* dynamic Raman spectroelectrochemistry has allowed us to study with high time-resolution the processes taking place for the activation of SERS substrates. Our results demonstrate the strong influence of the nanostructure electrogenerated during the electrochemical activation and the surface charge for the enhanced detection of cationic or anionic species. These findings challenge the consensus of using chloride-based electrolytes with the ORC method for the roughening and activation of SERS substrates. In specific conditions, the high enhancement factor of $1.8x10^{8}$ and the detection of pM concentrations agree with the feasible detection of only a few molecules in the solution. These results are achieved using a simple activation method and disposable substrates, thus opening the door to the possible detection of few or single-molecule events with user-friendly experiments.

Conflicts of interest

There are no conflicts to declare.

Notes and references

1 P. L. Stiles, J. A. Dieringer, N. C. Shah and R. P. Van Duyne, *Annu. Rev. Anal. Chem.*, 2008, **1**, 601–626.

2 H. M. Lee, S. M. Jin, H. M. Kim and Y. D. Suh, *Phys. Chem. Chem. Phys.*, 2013, **15**, 5276.

3 A. B. Zrimsek, N. Chiang, M. Mattei, S. Zaleski, M. O. McAnally, C. T. Chapman, A. Henry, G. C. Schatz and R. P. Van Duyne, *Chem. Rev.*, 2017, **117**, 7583–7613.

4 D. Graham and R. Goodacre, *Chem. Soc. Rev.*, 2008, **37**, 883.

5 X. Xie, H. Pu and D.-W. Sun, *Crit. Rev. Food Sci. Nutr.*, 2017, 1–14.

6 M. Fleischmann, P. J. Hendra and A. J. McQuillan, *Chem. Phys. Lett.*, 1974, **26**, 163–166.

7 J. E. Pemberton, A. L. Guy, R. L. Sobocinski, D. D. Tuschel and N. A. Cross, *Appl. Surf. Sci.*, 1988, **32**, 33–56.

8 K.-H. Yang, Y.-C. Liu and C.-C. Yu, *J. Mater. Chem.*, 2008, **18**, 4849.

9 J. J. Mock, M. Barbic, D. R. Smith, D. A. Schultz and S. Schultz, *J. Chem. Phys.*, 2002, **116**, 6755–6759.

10 J. Kneipp, H. Kneipp and K. Kneipp, *Chem. Soc. Rev.*, 2008, **37**, 1052.

11 D. Martín-Yerga, A. Pérez-Junquera, M. B. González-García, J. V. Perales-Rondon, A. Heras, A. Colina, D. Hernández-Santos and P. Fanjul-Bolado, *Electrochim. Acta*, 2018, **264**, 183–190.

12 V. S. Tiwari, T. Oleg, G. K. Darbha, W. Hardy, J. P. Singh and P. C. Ray, *Chem. Phys. Lett.*, 2007, **446**, 77–82.

13 C. Hamon and L. M. Liz-Marzán, *J. Colloid Interface Sci.*, 2018, **512**, 834–843.

14 J. P. Camden, J. a Dieringer, Y. Wang, D. J. Masiello, L. D. Marks, G. C. Schatz and R. P. Van Duyne, *J. Am. Chem. Soc.*, 2008, **130**, 12616–12617.

15 P. H. C. Camargo, L. Au, M. Rycenga, W. Li and Y. Xia, *Chem. Phys. Lett.*, 2010, **484**, 304–308.

16 W. Xie and S. Schlücker, *Chem. Commun.*, 2018, **54**, 2326–2336.

17 D.-Y. Wu, J.-F. Li, B. Ren and Z.-Q. Tian, *Chem. Soc. Rev.*, 2008, **37**, 1025.

18 F. Avila, C. Ruano, I. Lopez-Tocon, J. F. Arenas, J. Soto and J. C. Otero, *Chem. Commun.*, 2011, **47**, 4213.

19 D. P. dos Santos, G. F. S. Andrade, M. L. A. Temperini and A. G. Brolo, *J. Phys. Chem. C*, 2009, **113**, 17737–17744.

20 C. Han, L. Ge, C. Chen, Y. Li, Z. Zhao, X. Xiao, Z. Li and J. Zhang, *J. Mater. Chem. A*, 2014, **2**, 12594–12600.

21 W. Ji, X. Xue, W. Ruan, C. Wang, N. Ji, L. Chen, Z. Li, W. Song, B. Zhao and J. R. Lombardi, *Chem. Commun.*, 2011, **47**, 2426–2428.

22 R. A. Álvarez-Puebla, *J. Phys. Chem. Lett.*, 2012, **3**, 857–866.

23 A. Sivanesan, W. Adamkiewicz, G. Kalaivani, A. Kamińska, J. Waluk, R. Hołyst and E. L. Izake, *Electrochem. commun.*, 2014, **49**, 103–106.

24 E. C. Le Ru, E. Blackie, M. Meyer and P. G. Etchegoin, *J. Phys. Chem. C*, 2007, **111**, 13794–13803.

SUPPORTING INFORMATION

Towards single-molecule *in situ* electrochemical SERS detection with disposable substrates

Daniel Martín-Yerga, Alejandro Pérez-Junquera, María Begoña González-García, David Hernández-Santos, Pablo Fanjul-Bolado*

DropSens S.L. Edificio CEEI, Parque Tecnológico de Asturias, 33428 Llanera, Asturias, Spain

* Corresponding author: pfanjul@dropsens.com

EXPERIMENTAL

Instrumentation and electrodes

In situ dynamic Raman spectroelectrochemistry was performed using a compact and integrated instrument, SPELEC RAMAN (DropSens), which contains a laser source of 785 nm. This instrument was connected to a bifurcated reflection probe (DRP-RAMANPROBE) and a specific cell for screen-printed electrodes (DRP-RAMANCELL). The diameter of the laser spot was about 200 µm. This probe allows to get an average signal of a large surface area, and minimizes the irreproducibility produced by hot spots or non-active regions. The instrument was controlled by DropView SPELEC software, which allows to perform simultaneous and real-time spectroelectrochemical experiments, with totally synchronized data acquisition.

Screen-printed silver electrodes (DRP-C013, DropSens) were used throughout the work. These devices consist of a flat ceramic card on which a three-electrode system comprising the electrochemical cell is screen-printed. The working silver electrode is circular with a diameter of 1.6 mm, and the device has also an auxiliary electrode made of carbon and a silver electrode which acts as a pseudoreference. All spectroelectrochemical measurements were performed at room temperature and using a solution of 50 µL

for Raman, respectively. The reported potentials are related to the silver screen-printed pseudoreference electrode.

A JEOL 6610LV scanning electron microscope (SEM) was used to characterize the working silver electrodes at various stages of the electrochemical activation. This instrument was employed to record the energy-dispersive X-ray (EDX) spectra.

Reagents and solutions

Potassium ferricyanide, potassium chloride, potassium nitrate, lithium perchlorate, Tris(2,2-bipyridyl)dichlororuthenium(II) hexahydrate. Ultrapure water obtained with a Millipore DirectQ purification system from Millipore was used throughout this work.

Raman spectroelectrochemical measurements

Raman spectroelectrochemical experiments were performed by applying a linear sweep voltammetry in a range of potentials depending on the electrolyte employed at a scan rate of 50 mV/s, a step potential of 2 mV and equilibration time of 1 s. The potential range was from +0.3 to -0.4 V for chloride electrolytes and +0.5 to -0.4 V for non-chloride electrolytes. Raman spectra were registered with an integration time of 2 s and a laser power of 258 mW. In order to study the detection of ultralow concentrations, a chronoamperometric detection was used applying a potential of 0 V for 28 s after a previous activation with +0.40 V for 3 s. In this case, the Raman integration time was increased to 8 s in order to increase the number of scattered photons detected and the probability to detect them. Laser power was about 45 mW.

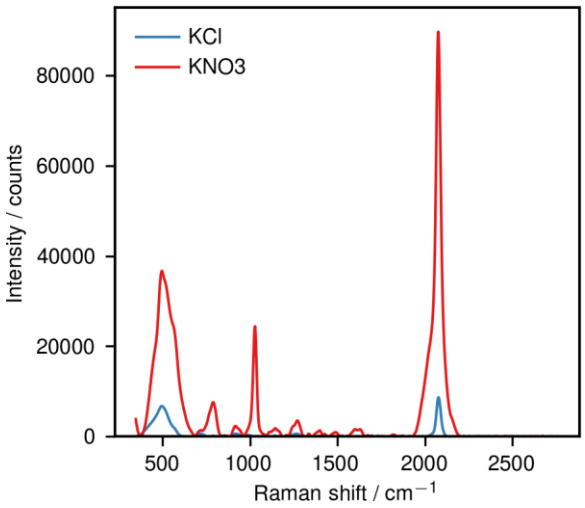

Figure S1. Spectra (baseline-corrected) obtained for 1x10^{-5} M ferricyanide after the substrate activation in KCl and KNO_3. Ferricyanide bands are observed in both experiments at 2076 and 495 cm^{-1}. Bands observed at 788 and 1028 cm^{-1} are due to nitrate vibrations, and they were not present in the KCl experiments. For the ferricyanide specific bands, the Raman shift of the peaks are similar in both experiments and the intensity increased for both peaks in KNO_3 at a similar extent. These facts suggest that the same kind of vibrations are involved in both experiments and the increment of the SERS signal is mainly due to the increased activity of the silver nanostructure. If the probe molecule interacts in a different orientation with the substrate, it would be expected some changes in the Raman shift or the intensity ratios between the two vibrational bands.

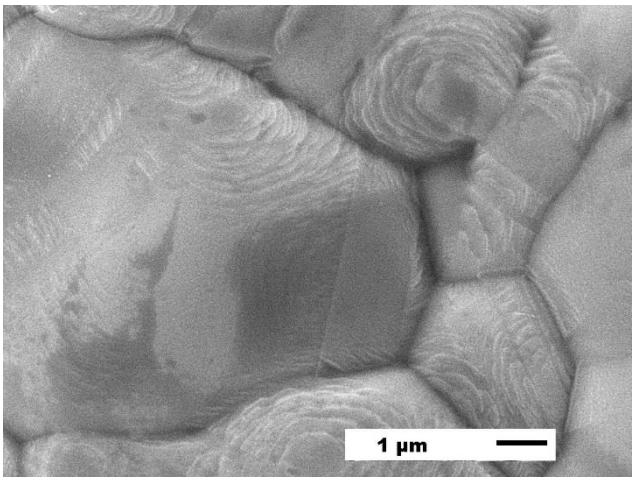

Figure S2. SEM image of the pristine surface of silver screen-printed electrode.

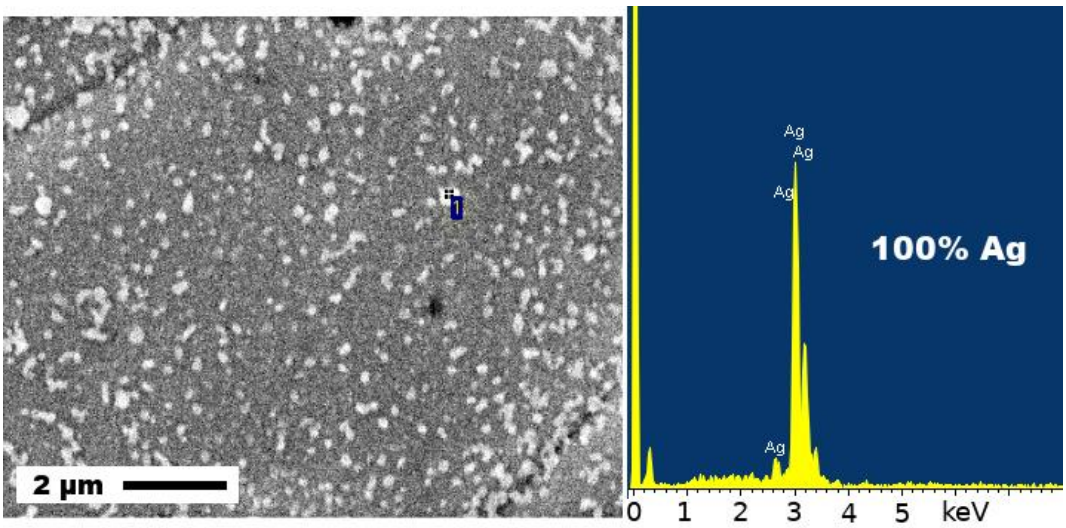

Figure S3. Representative SEM image of the silver screen-printed electrode after the *in situ* activation using KCl as electrolyte and EDX spectrum of one nanoparticle from the surface. This surface was obtained after the activation of the electrode from +0.3 V to -0.35 V, where the SERS signal was maximum. In this case, the voltammetric sweep was stopped when the AgCl generated initially has been reduced and elemental Ag is formed on the surface.

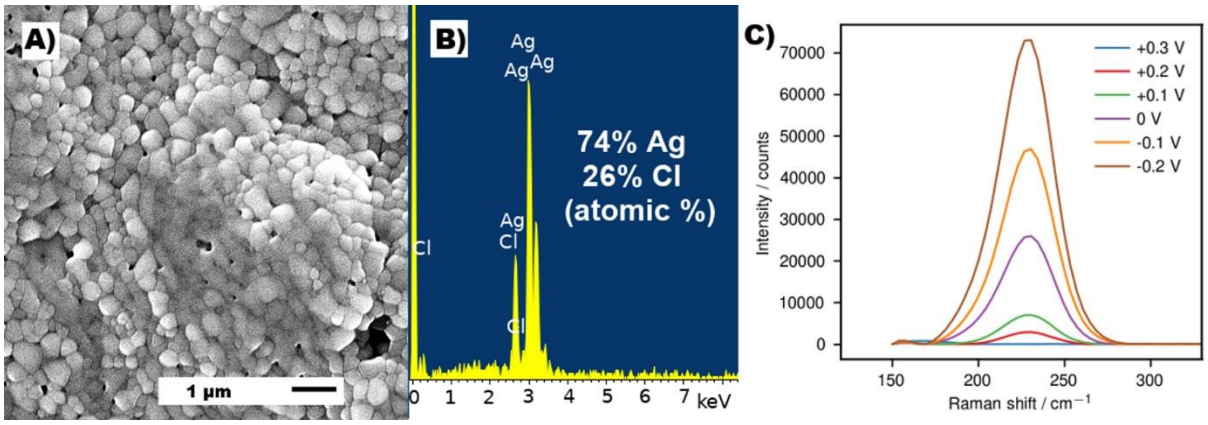

Figure S4. A) Representative SEM image of the silver screen-printed electrode after in situ activation from +0.3 V to +0.05 V using KCl as electrolyte and **B)** typical EDX spectrum of this surface. The electrochemical activation was stopped at potentials where only the oxidation of silver had occurred. The image shows a well-compacted surface composed of AgCl particles, which are generated after the oxidation of silver in presence of chloride ions. **C)** Raman spectra obtained between 150 and 300 cm^{-1} during the oxidation of the surface. The Raman band at 230 cm^{-1} increased during the oxidation step, confirming the generation of AgCl.

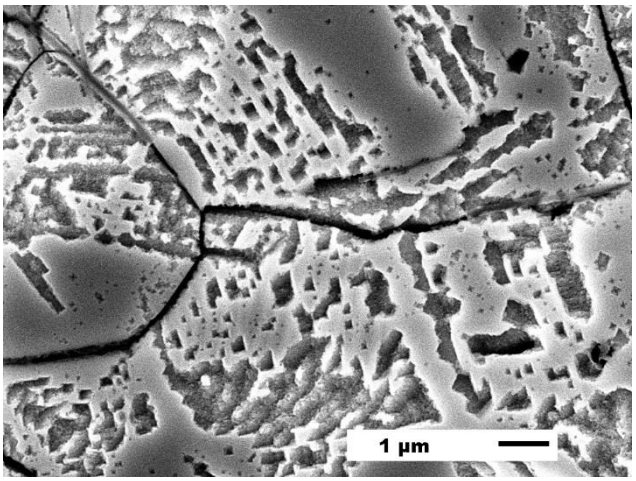

Figure S5. Representative SEM image of the silver screen-printed electrode after the *in situ* activation using KNO_3 as electrolyte. In this case, the voltammetric sweep was performed from +0.5 to +0.35 V (i.e. it was stopped during the oxidative stage). The initial silver electrode is oxidised resulting in an etched surface. This porous, rough surface seems to have a higher surface area than the initial pristine surface (see **Figure S2**), but this increment of the roughness did not increase the SERS signal. This fact suggests that this roughened silver is not SERS active and the increment of the surface area (visually observed) does not influence the SERS activity. The SERS signal only increased when fresh silver particles were generated during the reduction stage, demonstrating that the active surface area only comes from the new generated particles.

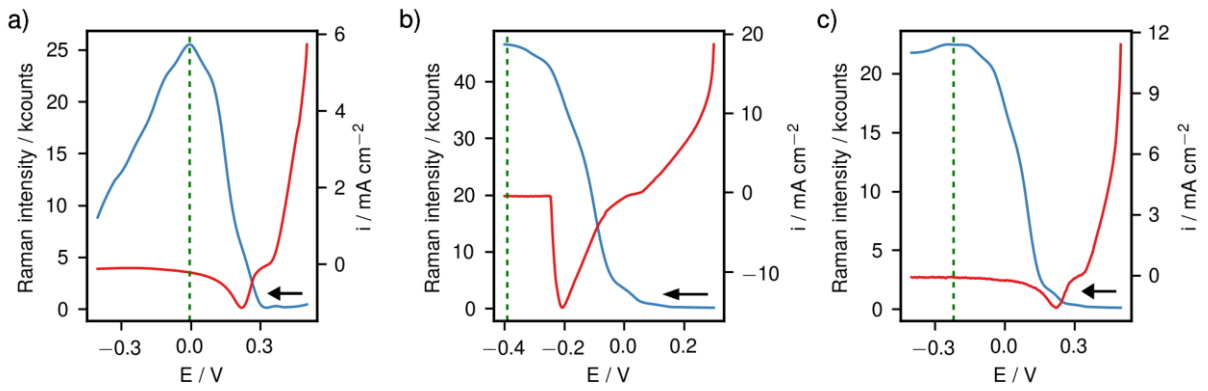

Figure S6. Evolution of the Raman peak intensity (baseline corrected) of different species (blue line) during the linear sweep voltammogram (red line) performed to activate the electrode surface with different electrolytes. Green lines show the potential for the maximum peak intensity. **A)** Peak intensity at 2076 cm^{-1} using a solution of $1x10^{-5}$ M $[Fe(CN)_6]^{3-}$ in 0.1 M $LiClO_4$. **B)** Peak intensity at 1036 cm^{-1} using a solution of $2x10^{-6}$ M $[Ru(bpy)_3]^{2+}$ in 0.1 M KCl. **C)** Peak intensity at 1036 cm^{-1} using a solution of $2x10^{-6}$ M $[Ru(bpy)_3]^{2+}$ in 0.1 M KNO_3.

The maximum peak intensity for $[Fe(CN)_6]^{3-}$ in 0.1 M $LiClO_4$ was c.a. 0 V. This case is similar to KNO_3 as the oxidation of silver does not form an insoluble product. This fact results in the reduction of soluble silver at more positive potentials than AgCl, and the maximum SERS effect after the generation of fresh silver is obtained c.a. 0 V. The SERS intensity in $LiClO_4$ was higher than that obtained in KCl, which seems to corroborate that the generation of fresh silver when the surface is charged more positively has a strong influence in the detection of anionic species such as $[Fe(CN)_6]^{3-}$ as observed for KNO_3 and KCl. In contrast, for cationic species such as $[Ru(bpy)_3]^{2+}$, the maximum SERS signal in a KCl electrolyte is obtained at about -0.4 V (30 mV more negative than $[Fe(CN)_6]^{3-}$). In KNO_3, the highest SERS signal was obtained at -0.20 V (about 200 mV more negative than $[Fe(CN)_6]^{3-}$), which corroborates that both the generation of fresh silver and the potential where the silver is generated influence the SERS signal of cationic and anionic species.

A) 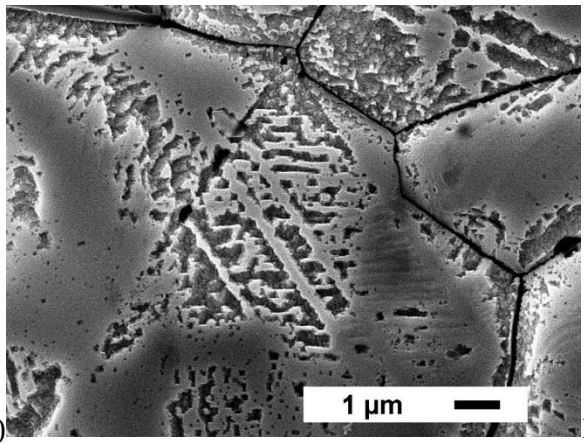

B) 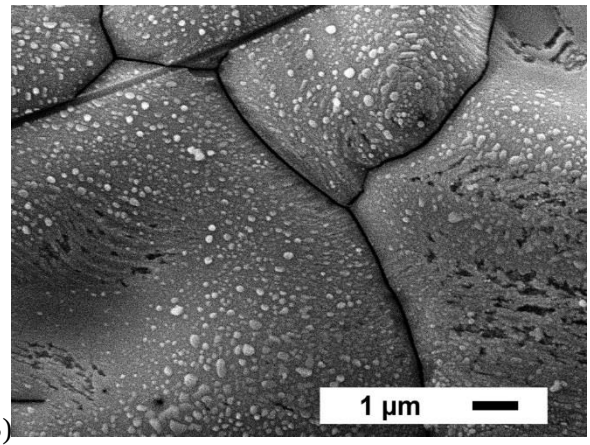

Figure S7. Representative SEM images of the electrode surface obtained during the electrochemical activation of the silver screen-printed electrode in presence of LiClO4. **A)** SEM image when the voltammetric sweep was recorded between +0.5 and +0.35 V (stopped during the oxidation stage) and **B)** SEM image when the voltammetric sweep was recorded between +0.5 and +0.0 V, where the SERS signal was maximum.

The electrode surface is also etched during the oxidation stage in a similar way to the experiment performed in KNO_3 because the silver is oxidised and soluble species are formed. No significant structural differences were visually found compared between both surfaces at these potentials. However, the cyclic voltammetry shows that the oxidation charge is significantly lower in presence of $LiClO_4$ compared to KNO_3. This fact has a significant impact on the structure of the generated particles during the reduction stage. In this case, a higher particle density but with smaller dimensions are found all over the surface as the amount of oxidised silver is lower. The different silver nanostructure seems to be fundamental to explain the different SERS signal in $LiClO_4$ or KNO_3 as the potential where the maximum SERS signal is obtained is very close for both electrolytes. It is also not unreasonable to think that the different adsorption of the electrolyte ions on the silver surface could have some influence on the SERS activity.

Estimation of the approximate number of detected molecules

We tried to estimate the approximate number of molecules that could be covering the silver surface during the SERS detection. The lowest detectable concentration of ferricyanide was $5x10^{-10}$ M, which in different units is $5x10^{-25}$ mol μm^{-3}. Converting this value to number of molecules using Avogadro's number, the lowest detectable concentration was 0.301 molecules μm^{-3}. The volume of solution detectable by SERS is defined by the spot diameter of the laser source, which is around 200 µm, and by the thickness of the solution where the molecules are in contact with the electrode surface. As shown in the main manuscript, the relationship between the concentration and the SERS intensity follows fairly well a Langmuir isotherm, which assumes that the surface is covered at most by a monolayer of the chemical probe. It is reasonable to think that at these ultralow concentrations the surface is not even covered by the complete monolayer. Therefore, the thickness of the detected volume is at most the thickness of a ferricyanide molecule. We performed computational calculations in order to estimate the thickness of a ferricyanide molecule strongly adsorbed on a silver surface. Avogadro software with Universal Force Field (UFF) was employed to optimize the molecular structure adsorbed on the silver surface. **Figure S8** shows the optimized geometry and the distance between the silver atom and the last nitrogen of the molecule, which was 0.823 nm. The estimated SERS detectable volume considering the laser spot diameter and the molecule coverage was 25.85 μm^3. Therefore, the number of molecules estimated in the detectable volume was 7.8 molecules. As mentioned, this is a rough calculation and several factors could influence this value: not all the electrode surface is covered by silver particles (this factor would lower the estimated number of molecules), it is well-known that nanostructures increase the surface area (this factor would increase the estimated number of molecules) and at the lower concentrations the probe molecules are probably in a sub-monolayer coverage (this factor would lower the estimated number of molecules). Therefore, these rough calculations, although approximate, seem to suggest that the detection of ferricyanide is very close to the single-molecule limit.

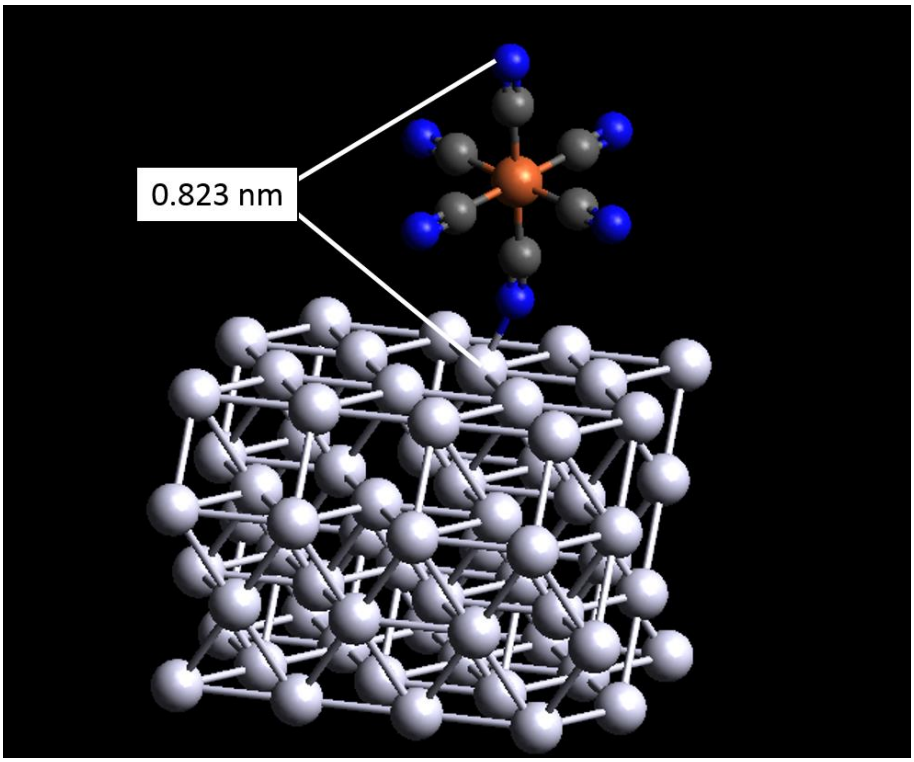

Figure S8. Schematic of the optimized structure of ferricyanide adsorbed on a silver surface illustrating the distance between the first silver atom of the substrate and the last nitrogen atom of the molecule.